
Integrin $\alpha_v\beta_3$ Imaging of Radioactive Iodine–Refractory Thyroid Cancer Using ^{99m}Tc -3PRGD2

Dan Zhao¹, Xiaona Jin¹, Fang Li¹, Jun Liang², and Yansong Lin¹

¹Department of Nuclear Medicine, Peking Union Medical College Hospital, Beijing, China; and ²Department of Oncology, the Affiliated Hospital of Qingdao University Medical College, Qingdao, China

Integrin $\alpha_v\beta_3$ has been proposed as a potential imaging target for radiolabeled RGD peptides and a molecular marker for the estimation of tumor angiogenesis, yet it has not been applied in differentiated thyroid cancer (DTC) patients with radioactive iodine–refractory (RAIR) lesions. The current study was conducted to assess the potential of integrin $\alpha_v\beta_3$ imaging in the detection of RAIR DTC lesions using ^{99m}Tc -PEG₄-E [PEG₄-c(RGDfK)]₂ (^{99m}Tc -3PRGD2), thus providing a feasible antiangiogenetic therapeutic target. **Methods:** Ten DTC patients (2 men, 8 women; mean age \pm SD, 56.4 \pm 9.8 y; age range, 42–73 y) with multiple RAIR metastases were recruited; all patients had both elevated thyroglobulin levels (thyroglobulin-positive) and negative ^{131}I whole-body scan (WBS) results. Clinical data were collected including history, ^{131}I WBS, contemporary CT, ultrasonography, thyroid-stimulating hormone, thyroglobulin, and antithyroglobulin. One or 2 target lesions were selected on the contemporary CT images using Response Evaluation Criteria in Solid Tumors 1.0 for all patients, 7 of whom were chosen for the calculation of the rates of lesion growth within the 3 mo before the study. WBS at 30 min and regional SPECT for lesions at 1 h were performed after the intravenous injection of ^{99m}Tc -3PRGD2. Two experienced nuclear medicine physicians read the images in a masked fashion. The tumor-to-background ratios were calculated for further analysis. **Results:** All the target RAIR metastatic lesions were identified as positive on ^{99m}Tc -3PRGD2 SPECT images. There was a significant correlation between the mean tumor-to-background ratios and mean growth rates of target lesions ($r = 0.878$, $P = 0.009$). **Conclusion:** The RAIR (^{131}I WBS–negative/thyroglobulin-positive) metastatic lesions can be traced using ^{99m}Tc -3PRGD2 imaging, meaning these lesions are highly neovascularized. ^{99m}Tc -3PRGD2 angiogenesis imaging can be used for the localization and growth evaluation of RAIR lesions, providing a new therapeutic target and a novel imaging modality to monitor the efficacy of certain antiangiogenetic therapy.

Key Words: ^{99m}Tc -3PRGD2; integrin $\alpha_v\beta_3$; refractory; differentiated thyroid cancer; SPECT

J Nucl Med 2012; 53:1872–1877

DOI: 10.2967/jnumed.112.107821

It is well known that differentiated thyroid cancer (DTC) includes papillary thyroid cancer and follicular thyroid cancer. Most DTC patients can survive disease-free for more than 30 y with appropriate surgery and radioactive iodine therapy. However, 2%–5% of these tumors will lose their differentiated phenotypes, develop a recurrent lack of avidity for radioactive iodine, and lead to the failure of ^{131}I treatment (1). These cases of DTC are commonly called radioactive iodine–refractory (RAIR) DTC, with negative ^{131}I whole-body scan results and elevated unstimulated thyroglobulin (>2.0 ng/mL, thyroglobulin-positive), indicating dedifferentiation of those lesions. RAIR DTC is prone to be more aggressive and metastatic, rendering cells that are more malignant and refractory, with a median patient survival of less than 5 y (2). Cancer guidelines of the American Thyroid Association recommend the use of ^{18}F -FDG PET/CT for the detection of RAIR DTC lesions. However, ^{18}F -FDG trapping is not tumor-specific, and at present in China most patients cannot afford the expense of ^{18}F -FDG PET for diagnosis, rather than treatment. A new cost-effective method for early detection and personalized therapy is highly desirable for these patients.

Integrin $\alpha_v\beta_3$ has been confirmed in various malignant tumors with high density, and it is essential for cell migration and invasion and plays an important role in tumor angiogenesis (3). Integrin $\alpha_v\beta_3$ expression is high on the surface of activated endothelial cells in newly formed blood vessels but is low in both resting endothelial cells and most normal organ systems, thus representing an interesting molecular marker for angiogenesis imaging (4). The adhesion of endothelial cells and extracellular matrix, mediated by integrin $\alpha_v\beta_3$, is vital for vascular endothelial growth factor receptor-2 activation (5). Ligands bearing RGD (Arg-Gly-Asp) peptide have a high affinity and specificity for integrin $\alpha_v\beta_3$, especially cyclic RGD dimmers with PEG₄ linkers (6). Unlike ^{18}F -FDG PET/CT as a diagnosis-only modality, integrin

Received Apr. 26, 2012; revision accepted Jul. 20, 2012.

For correspondence or reprints contact either of the following: Yansong Lin, Department of Nuclear Medicine, Peking Union Medical College Hospital, No. 1 Shuaifuyuan, Wangfujing St., Dongcheng District, Beijing, 100730, China.

E-mail: linyansong68@yahoo.com.cn

Jun Liang, Department of Oncology, the Affiliated Hospital of Qingdao University Medical College, No. 16 Jiangsu Rd., Shinan District, Qingdao, 266003, China.

E-mail: liangjun1959@yahoo.com.cn

Published online Oct. 15, 2012.

COPYRIGHT © 2012 by the Society of Nuclear Medicine and Molecular Imaging, Inc.

$\alpha_v\beta_3$ imaging by radiolabeled RGD peptide provides a specific method for visualizing tumor angiogenesis and a therapeutic target for antiangiogenic and antiintegrin drugs (7).

The RGD molecules ^{99m}Tc -NC100692, ^{18}F -P-PRGD2, ^{18}F -AH111585, and ^{18}F -galacto-RGD have already been used in the molecular imaging of cancer cell lines, animal models, or clinical cancer patients (including in murine osteosarcoma, human colon and renal adenocarcinoma, rat pancreatic tumors, ovarian carcinoma, human breast carcinoma, human glioblastoma, and human melanoma) to trace tumor angiogenesis and metastasis with PET or SPECT (8–13). The integrin $\alpha_v\beta_3$ expression level on tumor cell membranes correlates well with the RGD radiotracer tumor uptake on scintigraphy imaging (14). Compared with the ^{18}F -labeled tracers for PET, ^{99m}Tc -labeled nuclides are SPECT tracers that hold the advantage of being more broadly available. Moreover, the product can be kit-formulated and ready for routine clinical use with a simple, convenient labeling procedure and easy quality control. ^{99m}Tc -PEG₄-E [PEG₄-c(RGDfK)]₂ (^{99m}Tc -3PRGD2) is a new ^{99m}Tc -labeled cyclic RGD dimer peptide with increased receptor binding affinity and improved kinetics for the *in vivo* imaging of integrin $\alpha_v\beta_3$ expression in xenografted tumor-bearing models (6,15,16). The blood clearance kinetics, biodistribution, and radiation dosimetry of a kit-formulated ^{99m}Tc -3PRGD2 were also evaluated in nonhuman primates in our department, and no adverse reactions were observed to date (17). A multicenter study of ^{99m}Tc -3PRGD2 for integrin receptor imaging of lung cancer was sponsored by our department last year. To date, RGD molecular imaging including ^{99m}Tc -3PRGD2 has not been used in thyroid cancer, in particular ^{131}I WBS-negative/thyroglobulin-positive patients. This study provides clinical integrin imaging data for RAIR DTC.

MATERIALS AND METHODS

Study Design and Patient Recruitment

The study protocol was approved by the ethics committee of Chinese Academy of Medical Sciences and Peking Union Medical College Hospital (PUMCH) and by the institutional review boards of the PUMCH. Written informed consent was obtained from all subjects. Subject inclusion was based on the following presumptive diagnosis criteria: age over 18 y; a negative pregnancy test; clinically acceptable renal and hepatic function (as judged by an investigator according to blood examinations); and RAIR DTC patients with metastatic lesions, treated by radioactive iodine many times, who were ^{131}I WBS-negative/thyroglobulin-positive. In addition, other findings from clinical staging procedures served as the standard of reference (including anti-thyroglobulin levels, ^{18}F FDG PET/CT, bone scintigraphy, contemporary CT, and ultrasonography). Because of ethical concerns, biopsies and histopathology were not available for most of the analyzed metastases. The exclusion criteria included ^{131}I WBS positivity, thyroglobulin negativity, pregnancy, lactation, and impaired renal or liver function.

Ten RAIR DTC patients (2 men, 8 women; mean age \pm SD, 56.4 \pm 9.8 y; age range, 42–73 y; median body weight \pm SD, 65.7 \pm 12.8 kg [weight range, 44.0–87.5 kg]) were recruited from the Nuclear Medicine Department of PUMCH.

The protocol outlined admission, dosing, and safety checks on the same day up to 2.5 h after the administration of ^{99m}Tc -3PRGD2. Imaging and safety assessments were performed during the first 2.5 h after injection, after which the subjects were allowed to leave the site.

Radiosynthesis of ^{99m}Tc (Hydrazinonicotinamide-3PRGD2)(Tricine) (TPPTS) and Agent Injection

All chemicals obtained commercially were of analytic grade and used without further purification. Succinic acid, trisodium triphenylphosphine-3,3',3''-trisulfonate (TPPTS), and tricine were purchased from Sigma-Aldrich. Cyclic RGD peptide dimer 3PRGD2 was custom-made by Peptides International, Inc. $\text{Na}^{99m}\text{TcO}_4$ was obtained from a commercial $^{99}\text{Mo}/^{99m}\text{Tc}$ generator (Beijing Atom High Tech Co., Ltd.). Synthesis of the labeling precursor, kit preparation, and subsequent ^{99m}Tc labeling were performed as previously described (17). Briefly, the kit for preparation of ^{99m}Tc -3PRGD2 was formulated by combining 20 μg of hydrazinonicotinamide-3PRGD2, 5 mg of TPPTS, 6.5 mg of tricine, 40 mg of mannitol, 38.5 mg of disodium succinate hexahydrate, and 12.7 mg of succinic acid. For ^{99m}Tc radiolabeling, the kit vial was added to 1 mL of $^{99m}\text{TcO}_4$ -saline solution (1,110–1,850 MBq [30–50 mCi]) and then water-bathed at 100°C for 20 min. The resulting solution was analyzed by instant thin-layer chromatography using Gelman Sciences silica-gel paper strips and a 1:1 mixture of acetone and saline as eluant. For clinical use, the radiochemical purity was always greater than 95%. The reaction mixture was then diluted to 370 MBq (10 mCi) per milliliter with saline and filtered with a 0.20- μm Millex-LG filter (EMD Millipore). Each patient was injected with ^{99m}Tc -3PRGD2 (11.1 MBq/kg [0.3 mCi/kg]). Before imaging, all the subjects were asked to urinate completely.

Imaging Protocols

With the patients' arms laid beside their body, anterior and posterior planar scans of the whole body were started at 30 min after injection, using a dual-head γ -camera with low-energy high-resolution collimators and a 20% energy acceptance window centered on 140 keV. SPECT and coregistered spiral CT were performed at 1 h after injection with the same γ -camera. The speed of whole-body scanning was set at 10 cm/min, followed by SPECT (zoom, $\times 1$; 60 s/frame/12°; 30 steps/360°) with the patients' arms raised above their head. The images were obtained using the optimized parameters of the Philips Precedence SPECT system. The DICOM image files of each patient were saved and transferred to Extended Brilliance workspace NM1.0 (Philips) for centralized reconstruction, reading, and analysis.

Image Analysis

The ^{99m}Tc -3PRGD2 images were evaluated by 2 experienced nuclear medicine physicians through consensus reading masked to the source, history, and pathologic conditions of the patients. For analysis, 1 or 2 target lesions were selected and measured by the Response Evaluation Criteria in Solid Tumors (RECIST) 1.0 (18). The total number of selected target lesions was 18, and they were all negative on ^{131}I WBS. The variations of lesion sizes were documented, and the mean growth rates of target lesions for 7 patients in the 3 mo before the study were calculated and recorded (dynamic follow-up of CT images in the past 3 mo were not available for the other 3 patients). Tumor-to-background (T/B) ratios of target lesions on SPECT were measured and calculated by the

same person using a consistent standard. Briefly, on the section on which target lesions were measured according to RECIST 1.0, regions of interest (ROI) were drawn on the entire target lesions on SPECT cross-sections. And on the same section, a blood-pool background ROI with a diameter of 20 mm was set over the contralateral normal lung tissue or surrounding normal soft tissue. The T/B ratios were calculated by mean counts of the tumor ROI divided by mean counts of the background ROI.

Statistics Analysis

All quantitative data were expressed as mean \pm SD. The correlation between mean T/B ratios and mean growth rates of the target lesions was evaluated by linear regression analysis and by calculation of the Pearson correlation coefficient *r*. Statistical significance was tested using SPSS (version 19.0; IBM) at the level of 0.01.

RESULTS

Distribution of ^{99m}Tc-3PRGD2 in Human Body

The image quality of ^{99m}Tc-3PRGD2 scans was good for all 10 enrolled patients. The distribution of ^{99m}Tc-3PRGD2 in the human body could be observed clearly on the anterior and posterior whole-body images (Fig. 1C). Except for the intense accumulation in the kidneys and bladder corresponding to the main excretion pathway, there was moderate ^{99m}Tc-3PRGD2 uptake in the liver, spleen, intestines, nasopharyngeal region, and bone marrow. Because pulmonary metastases account for more than 50% of thyroid cancer metastases (19), the low background in the lungs and mediastinum allowed for easy discrimination of thoracic lesions.

Evaluation for ^{99m}Tc-3PRGD2 Imaging of Target Metastatic RAIR Lesions in DTC Patients

The characteristics of enrolled patients are shown in Table 1. All 18 selected target lesions were identified on SPECT images with the prescribed ^{99m}Tc-3PRGD2 administration imaging protocol. The mean T/B ratio of all 18 target lesions was 5.2 ± 2.8 . A statistically significant correlation was found between the mean T/B ratios and mean growth rates of target lesions, with a correlation coefficient of 0.878 ($P = 0.009$) (Fig. 2). Figure 1 illustrates the var-

iations of TSH, thyroglobulin, and antithyroglobulin levels; negative ¹³¹I WBS results with TSH stimulation; and positive ^{99m}Tc-3PRGD2 planar and SPECT images of RAIR lesions in patient 1.

DISCUSSION

The management of RAIR DTC metastatic lesions has caused a dilemma. Surgery is not eligible for multiple metastases. Neither ¹³¹I WBS for early detection nor radioactive iodine for effective therapy works because RAIR lesions usually lose the ability to concentrate ¹³¹I. RAIR cancer cells proliferate quickly, leading to active metabolism and the lack of oxygen, with vigorous angiogenesis and higher expression of glut protein on the cell membrane (20). ¹⁸F-FDG PET/CT, an imaging technique based on the high expression of glut protein, provides unique information about the molecular and glucose metabolic changes associated with DTC. The guidelines of the American Thyroid Association recommend that if an empiric dose (3.7–7.4 GBq [100–200 mCi]) of radioactive iodine fails to localize the persistent disease, ¹⁸F-FDG PET/CT should be considered, especially in DTC patients with stimulated serum thyroglobulin levels greater than 10–20 ng/mL or in those with aggressive histologies, to localize metastatic lesions that may require treatment or continued close observation (21). However, it is important to realize that ¹⁸F-FDG trapping is not tumor-specific. Both malignant thyroid tumors and some benign thyroid diseases, such as Graves disease and hyperactive thyroid adenoma, can take up ¹⁸F-FDG. Moreover, cervical lymph nodes with inflammation or other inflamed tissues could show high ¹⁸F-FDG uptake on the PET scans (22). At present in China, SPECT is more widely available than PET. Radiotracers for SPECT are easier to prepare and usually have a longer half-life than those for PET. Most patients cannot afford the expense of ¹⁸F-FDG PET for diagnosis, rather than treatment. A new SPECT agent with a therapeutic target is urgently needed both for diagnosing and for guiding further treatment.

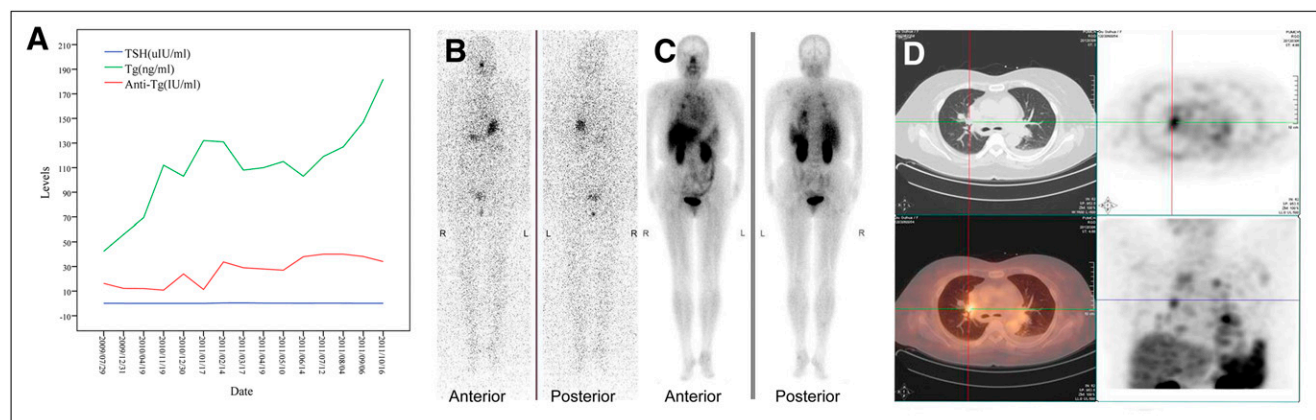


FIGURE 1. Elevated levels of unstimulated thyroglobulin (ng/mL) and antithyroglobulin (IU/mL) with corresponding TSH (A), ¹³¹I-negative image with TSH stimulation (TSH > 30 μ IU/mL) (B), and RGD-positive planar (C) and SPECT images (D). Tg = thyroglobulin.

TABLE 1
Patient Characteristics (*n* = 10)

Patient no.	Pathologic type	No. of radioactive iodine therapy administrations		Accumulated dose		Target lesions		¹³¹ I WBS	Mean thyroglobulin ± SD (ng/mL)*	Mean antithyroglobulin ± SD (IU/mL)	Mean growth rate of target lesions in 3 mo before study (mm/mo)	SPECT image (mean T/B ratio of target lesions)
		GBq	mCi	Site	Total no.							
1	PTC (follicular subtype)	5	29.6	800	Lung	2	Negative	110.4 ± 34.9	25.6 ± 11.4	0.998	9.8	
2	FTC	7	33.3	900	Lung	2	Negative	>1,000	47.4 ± 6.0	0.317	3.7	
3	FTC	6	37	1,000	Lung	2	Negative	>1,000	29.6 ± 3.4	0.463	8.1	
4	PTC (follicular subtype)	3	16.65	450	Mediastinum	1†	Negative	128.7 ± 18.8	20.3 ± 0.4	NA‡	6.5	
5	PTC (follicular subtype)	1	7.4	200	Lung	2	Negative	>1,000	38.3 ± 0.1	NA‡	5.4	
6	PTC (follicular subtype)	7	40.7	1,100	Bone and lymph nodes in pelvis	2	Negative	42.9 ± 23.1	34.1 ± 6.4	0.140	3.3	
7	PTC	3	16.65	450	Lung	1†	Negative	0.5 ± 0.6	59.4 ± 10.4	0.403	5.3	
8	PTC	2	11.1	300	Lung	2	Negative	26.9 ± 5.3	12.8 ± 2.8	NA‡	4.6	
9	PTC	5	33.3	900	Lung	2	Negative	481.2 ± 256.9	39.0 ± 75.0	0.350	3.7	
10	PTC	1	7.4	200	Bone	2	Negative	>1,000	118.5 ± 77.7	0.250	2.0	

*Levels of serum thyroglobulin sometimes are interfered with by antithyroglobulin levels. Combination of the 2 is taken into consideration when thyroglobulin level stays normal while antithyroglobulin level stays high.

†Patients 4 and 7 had only 1 lesion analyzed because these patients had only 1 evaluable lesion according to RECIST 1.0.

‡Dynamic follow-up of CT images in 3 mo before study was not available.

PTC = papillary thyroid cancer; FTC = follicular thyroid cancer.

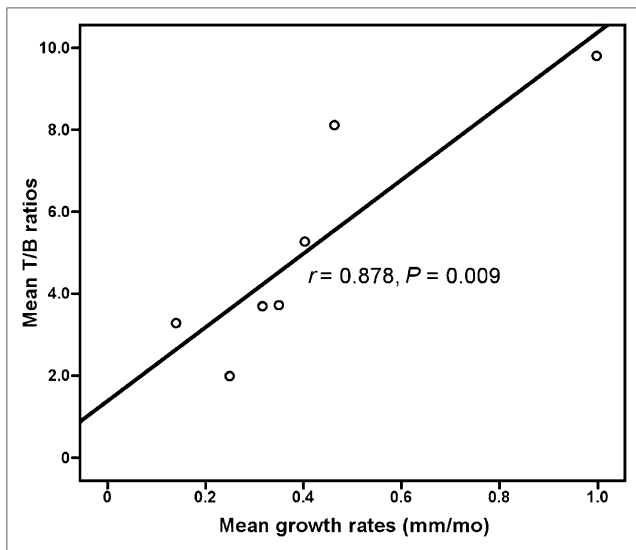


FIGURE 2. Correlation of mean T/B ratios and mean growth rates. Statistically significant correlation is found between mean T/B ratios and mean growth rates of target lesions, with correlation coefficient of 0.878 ($P = 0.009$).

^{99m}Tc -3PRGD2, a novel specific radiotracer for targeting integrin $\alpha_v\beta_3$, has been selected as a candidate for clinical evaluations because of its high uptake, long retention time, and high metabolic stability in athymic nude mice bearing U87MG gliomas and MDA-MB-435 breast cancer xenografts (6,15). ^{99m}Tc -3PRGD2 has recently been translated into clinical trials following its preliminary applications and several other RGD-based tracers' applications in preclinical experiments and clinical trial (10–12,15). A multicenter study of ^{99m}Tc -3PRGD2 for integrin receptor imaging of lung cancer was organized by our department last year, and results indicated that ^{99m}Tc -3PRGD2 imaging at 1 h was sensitive enough for the detection of lung cancer, with a sensitivity of 88% for semiquantitative analysis that could reach 93%–97% in visual analysis when considering the volume effect, necrosis, and metastasis (23). The present study is the first application of RGD imaging in DTC patients with RAIR lesions. On the planar images, the distribution of ^{99m}Tc -3PRGD2 in the human body could be observed clearly, presenting the same results as those in lung cancer patients. Except for the intense accumulation in the kidneys and bladder corresponding to the main excretion pathway, there was moderate ^{99m}Tc -3PRGD2 uptake in the liver, spleen, intestines, nasopharyngeal region, and bone marrow. On the SPECT images, all target lesions could be identified as positive, with various higher uptake of ^{99m}Tc -3PRGD2 than blood-pool background, contrary to their negative uptake demonstrated by ^{131}I WBS. The mean T/B ratio of all target lesions was 5.2 ± 2.8 . To reflect the recent status of tumor growth, the mean growth rates of target lesions in 7 patients in the 3 mo before the study were calculated and recorded (dynamic follow-up of CT images in the past 3 mo were not available for the other 3 patients). The

mean T/B ratios of target lesions escalated as the mean growth rates increased, and significant correlation was found between the two ($r = 0.878$, $P = 0.009$) (Fig. 2). The correlation suggests that active angiogenesis with higher integrin $\alpha_v\beta_3$ density on RAIR DTC cells and tumor neovasculature is needed for rapid growth of tumor lesions. The higher the ^{99m}Tc -3PRGD2 uptake is in target lesions, the more rapid is the tumor growth, and vice versa. ^{99m}Tc -3PRGD2 also holds promise for monitoring response to antiangiogenic therapy, as demonstrated by other RGD molecules (7,24).

Further analysis illustrates that all the lesions larger than 1 cm were observed clearly on ^{99m}Tc -3PRGD2 SPECT images. Among these lesions, some presented higher uptake whereas others presented relatively lower uptake. Not all of the lesions smaller than 1 cm were detected. The major cause of this phenomenon is the heterogeneous property of the tumor itself; however, partial-volume effects in small lesions may be another reason. Six of 10 patients had undergone an ^{18}F -FDG PET/CT scan. Integrin imaging was in accordance with ^{18}F -FDG uptake in almost all of the individual metastatic lesions larger than 1 cm (which is a limitation of SPECT because of poor resolution). The metastatic RAIR DTC lesions can have both a high glucose metabolic rate and vigorous angiogenesis. The comparison of ^{99m}Tc -3PRGD2 with ^{18}F -FDG PET/CT and further monitoring of its therapeutic efficacy are in progress.

CONCLUSION

In this study, significant uptake of ^{99m}Tc -3PRGD2 could be observed in RAIR DTC lesions, contrary to their negative ^{131}I WBS results. A correlation between the mean T/B ratios and mean growth rates of lesions was confirmed, indicating active angiogenesis and malignant phenotypes of RAIR DTC. ^{99m}Tc -3PRGD2 with SPECT is a promising modality for diagnosing and guiding further treatment of RAIR DTC.

DISCLOSURE STATEMENT

The costs of publication of this article were defrayed in part by the payment of page charges. Therefore, and solely to indicate this fact, this article is hereby marked "advertisement" in accordance with 18 USC section 1734.

ACKNOWLEDGMENTS

No potential conflict of interest relevant to this article was reported.

REFERENCES

- Rivera M, Ghossein RA, Schoder H, et al. Histopathologic characterization of radioactive iodine-refractory fluorodeoxyglucose-positron emission tomography-positive thyroid carcinoma. *Cancer*. 2008;113:48–56.
- Carr LL, Mankoff DA, Goulart BH, et al. Phase II study of daily sunitinib in FDG-PET-positive, iodine-refractory differentiated thyroid cancer and metastatic medullary carcinoma of the thyroid with functional imaging correlation. *Clin Cancer Res*. 2010;16:5260–5268.
- Hood JD, Cheresh DA. Role of integrins in cell invasion and migration. *Nat Rev Cancer*. 2002;2:91–100.

4. Zhou Y, Chakraborty S, Liu S. Radiolabeled cyclic RGD peptides as radiotracers for imaging tumors and thrombosis by SPECT. *Theranostics*. 2011;1:58–82.
5. Soldi R, Mitola S, Strasly M, et al. Role of $\alpha v \beta 3$ integrin in the activation of vascular endothelial growth factor receptor-2. *EMBO J*. 1999;18:882–892.
6. Wang L, Shi JY, Kim YS, et al. Improving tumor-targeting capability and pharmacokinetics of ^{99m}Tc -labeled cyclic RGD dimmers with PEG₄ linkers. *Mol Pharm*. 2009;6:231–245.
7. Morrison MS, Ricketts SA, Barnett J, et al. Use of a novel Arg-Gly-Asp radioligand, ^{18}F -AH111585, to determine changes in tumor vascularity after anti-tumor therapy. *J Nucl Med*. 2009;50:116–122.
8. Liu Z, Liu SL, Wang F, et al. Noninvasive imaging of tumor integrin expression using ^{18}F -labeled RGD dimer peptide with PEG₄ linkers. *Eur J Nucl Med Mol Imaging*. 2009;36:1296–1307.
9. Axelsson R, Bach-Gansmo T, Castell-Conesa J, et al. An open-label, multicenter, phase 2a study to assess the feasibility of imaging metastases in late-stage cancer patients with the alpha v beta 3-selective angiogenesis imaging agent ^{99m}Tc -NC100692. *Acta Radiol*. 2010;51:40–46.
10. Bach-Gansmo T, Danielsson R, Saracco A, et al. Integrin receptor imaging of breast cancer: a proof-of-concept study to evaluate ^{99m}Tc -NC100692. *J Nucl Med*. 2006;47:1434–1439.
11. Beer AJ, Lorenzen S, Metz S, et al. Comparison of integrin $\alpha v \beta 3$ expression and glucose metabolism in primary and metastatic lesions in cancer patients: a PET study using ^{18}F -galacto-RGD and ^{18}F -FDG. *J Nucl Med*. 2008;49:22–29.
12. Kenny LM, Coombes RC, Oulie I, et al. Phase I trial of the positron-emitting Arg-Gly-Asp (RGD) peptide radioligand ^{18}F -AH111585 in breast cancer patients. *J Nucl Med*. 2008;49:879–886.
13. Haubner R. $\alpha v \beta 3$ -integrin imaging: a new approach to characterize angiogenesis? *Eur J Nucl Med Mol Imaging*. 2006;33(suppl 1):54–63.
14. Haubner R, Weber WA, Beer AJ, et al. Noninvasive visualization of the activated $\alpha v \beta 3$ integrin in cancer patients by positron emission tomography and [^{18}F] galacto-RGD. *PLoS Med*. 2005;2:e70.
15. Zhou Y, Kim YS, Chakraborty S, et al. ^{99m}Tc -labeled cyclic RGD peptides for non-invasive monitoring of tumor integrin $\alpha v \beta 3$ expression. *Mol Imaging*. 2011;10:386–397.
16. Liu ZF, Jia B, Shi JY, et al. Tumor uptake of the RGD dimeric probe ^{99m}Tc -G3-2P4-RGD2 is correlated with integrin expressed on both tumor cells and neovasculature. *Bioconj Chem*. 2010;21:548–555.
17. Jia B, Liu ZF, Zhu ZH, et al. Blood clearance kinetics, biodistribution, and radiation dosimetry of a kit-formulate integrin $\alpha v \beta 3$ -selective radiotracer ^{99m}Tc -3PRGD in non-human primates. *Mol Imaging Biol*. 2011;13:730–736.
18. Therasse P, Arbuck GS, Eisenhauer AE, et al. New guidelines to evaluate the response to treatment in solid tumors. *J Natl Cancer Inst*. 2000;92:205–216.
19. Ruegamer JJ, Hay ID, Bergstralh EJ, et al. Distant metastases in differentiated thyroid carcinoma: a multivariate analysis of prognostic variables. *J Clin Endocrinol Metab*. 1988;67:501–508.
20. Antonelli A, Ferri C, Ferrari SM, et al. New targeted molecular therapies for dedifferentiated thyroid cancer. *J Oncol*. 2010;2010:921682.
21. Cooper DS, Doherty MG, Haugen RB, et al. Revised American thyroid association management guidelines for patients with thyroid nodules and differentiated thyroid cancer. *Thyroid*. 2009;19:1167–1214.
22. Liu Y. Clinical significance of thyroid uptake on ^{18}F -fluorodeoxyglucose positron emission tomography. *Ann Nucl Med*. 2009;23:17–23.
23. Zhu Z, Miao WB, Li QW, et al. ^{99m}Tc -3PRGD2 for integrin receptor imaging of lung cancer: a multicenter study. *J Nucl Med*. 2012;53:716–722.
24. Jung KH, Lee KH, Paik JY, et al. Favorable biokinetic and tumor-targeting properties of ^{99m}Tc -labeled glucosamino RGD and effect of paclitaxel therapy. *J Nucl Med*. 2006;47:2000–2007.